Gaussian Process Regression in Prediction Wheelchair Propulsion Kinematics

Erivelton Gualter dos Santos[†], Lexie Mallinos[†]
[†] Ph.D Candidate, Cleveland State University
[‡] Ph.D Student, Cleveland State University

Abstract. The 3D motion capture data of the wheelchair propulsion can be used to calculate the joint angles of the elbow and shoulder. A Gaussian process regression can be applied to this data to accurately calculate and predict the forces and moments applied to the wheel itself. By comparing the actual data of the wheelchair sensor to that that was predicted by the Gaussian model, this stochastic methodology can be a reliable and accurate way to obtain the necessary wheelchair kinematics that make it possible to better understand and improve wheelchair design.

1. Introduction

Advancements in technology and motion capture software makes it possible to develop an in depth look into the biomechanics of human movement. In particular, motion capture technology has allowed researchers to analyze unique locomotion applications such as manual wheelchair propulsion. Despite the significant portion of the population that relies on wheelchairs, manual wheelchair use results in injuries to the arms and shoulders due to their low efficiency and high energy demand (Ackermann et al., 2015; Boninger et al., 2002; Cooper & Quatrano, 1999; Van der Woude et al., 2001). Furthermore, this energy inadequacy is a result of the "radial component of the push force during the propulsion phase, based on the fact that only the tangential component of the force on the rim contributes to the moment applied to the wheel," thus resulting in forward propulsion (Ackermann et al., 2015).

Fraction Effective Force (FEF) is used to determine how effective the wheelchair propulsion will be by quantifying the tangential component of the total pushrim force. Unfortunately, the literature has measured low FEF ratios even in experienced users (Kotajarvi et al., 2004; Veeger et al., 1991). As a result, the FEF is the only force that will contribute to the mechanical work whereas the radial forces are a result of the "musculoskeletal structure and mechanical constraints imposed by the wheelchair-user system" (Ackermann et al., 2015). In order to improve the experience for wheelchair users, it is important to understand the biomechanics behind wheelchair operation so that future designs can be optimized to increase efficiency and reduce energy expenditure for the user.

Understanding the motion capture data is imperative in order to accurately quantify shoulder and elbow kinetics and kinematics of wheelchair users. However, current methodologies rely on using anthropometric data to determine the body segment lengths, mass, center of mass, and radius of gyration for each segment. Although useful, this data is an approximation of the actual measurements of the subject and are based on averages. Thus, the biomechanics that are calculated from these measurements experience a small degree of error and do not accurately reflect the in vivo biomechanics. As such, stochastic processes such as Bayesian and Gaussian inferences make it possible to determine and optimize the anthropometric measurements to reflect the data obtained during motion capture.

Through the utilization of data obtained from wheelchair locomotion three-dimensional (3D) motion capture, it is possible to measure the force and moments applied to the wheel using instrumented wheels with torque/force load cells such as SmartWheel (Out-Front, Mesa, AZ, USA). However, due to the high cost of this equipment, it is not a practical and economical resource that can be available to all. In this context, the aim of this paper is to propose a method to estimate the forces and moments applied to the elbow and shoulder from 3D motion capture data. In doing so, this report presents a Gaussian process regression to estimate the forces and moments applied to the wheelchair based on these joint coordinates.

2. Methods

2.1. **Data Collection.** In this section, we describe our experimental design to collect the wheelchair propulsion task (dos Santos, 2017). Wheelchair motion capture data was obtained in collaboration with the *BMClab - Biomechanics and Motor Control Laboratory* of the Biomedical Engineering program at the Federal University of ABC. This series of experiments involved the participant operating the wheelchair at a normal velocity where the following data was captured: 1) Force and moment signals during the propulsion from the wheelchair wheel; 2) EMG signals from a variety of muscles during the propulsion; and 3) 3D position of the markers. A system with 12 cameras with 4 Mb of resolution at 200 Hz (Motion Analysis, Santa Rosa, CA) records the position of these markers (Figure 1). An instrumented wheelchair wheel (Out-Front, Mesa, AZ, USA) collects the force and moments applied to the push-rims. Last, a wireless EMG system with 10 sensors (Delsys, Natick, Massachusetts) measures the muscle activation.

Figure 3 shows a total of 26 reflective markers are placed on the users, respecting the International Biomechanical Society's recommendations (Wu et al., 2005), which is described in (Jaimes, 2016). Additionally, two markers are placed on the wheel's center, one for each rear wheel, on the axle.

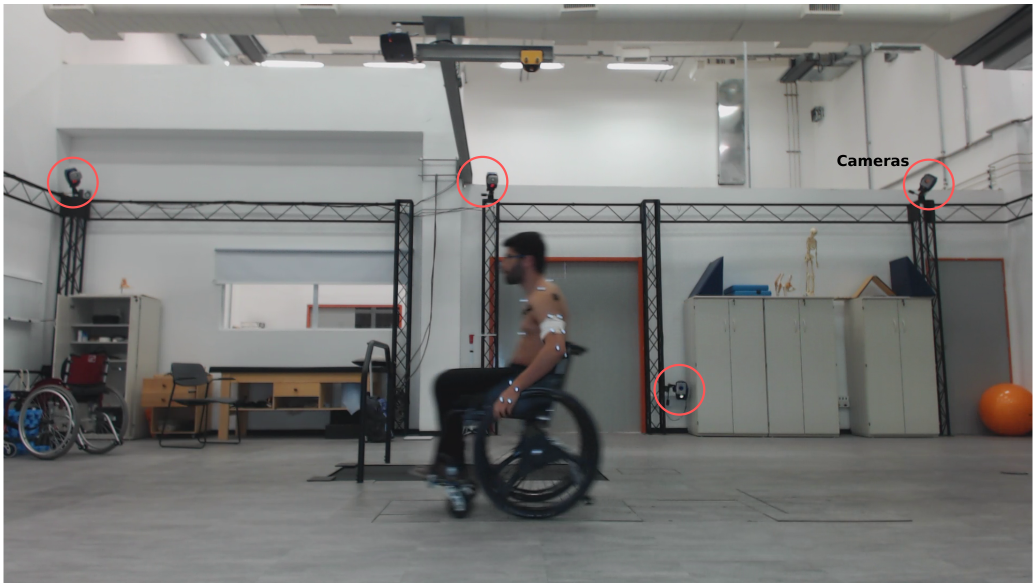

Figure 1. Laboratory "set up".

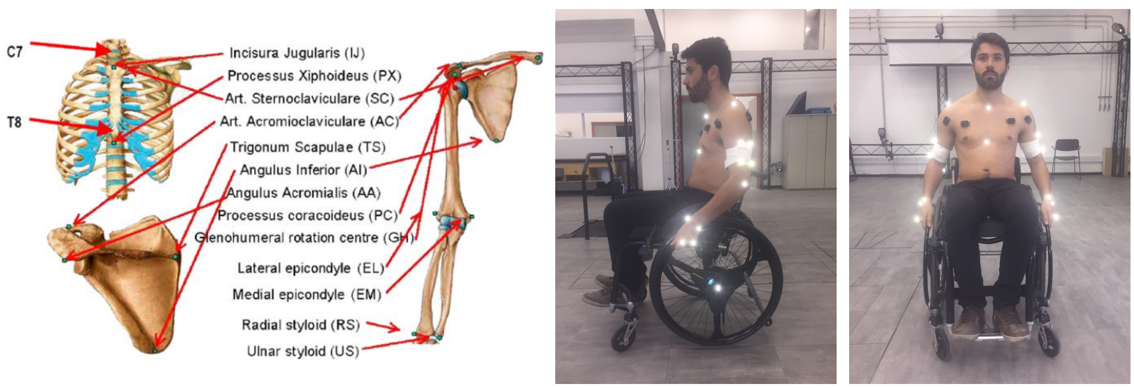

Figure 2. Location Makers.

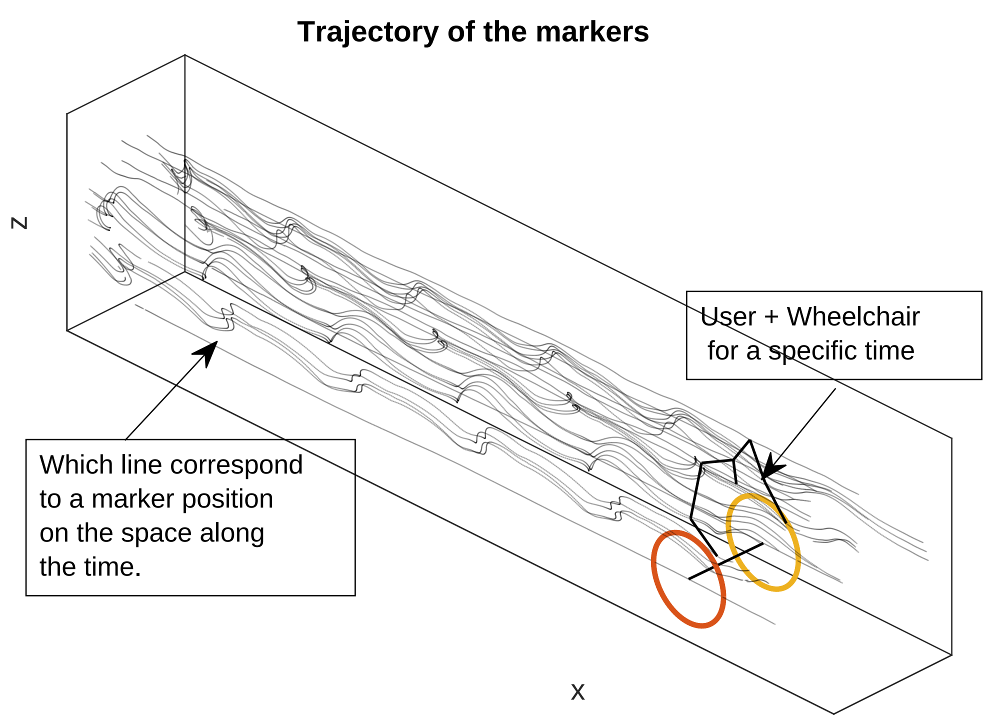

A total of 8 trials were performed: 2x warm-up session (free wheelchair driving), 3x Normal velocity during the propulsion, 3x Maximal velocity during the propulsion, and 2x deceleration experiment. Each trial record consist in several data that is required to be synchronized and interpolated at a 240Hz frequency. These generated data described in the following is saved in independent files:

- **SW1-0X.csv**: Force and moment data for the left wheel;
- **SW2-0X.csv**: Force and moment data for the right wheel;
- **mwX.anc**: Analog signals to synchronize the SmartWheel and motion capture analysis;
- **wcX-Delsys.csv** : EMG data;
- **wcX.trc** : Position of markers placed on a subject at different times during a motion capture trial;

2.2. **Mathematical Description of Wheelchair-User Dynamics.** The model of the planar wheelchair-user system developed by Ackermann et al. (Ackermann et al., 2015) was utilized for this experiment. This model defines the arms as four rigid bodies of bilateral symmetry with the elbow and shoulder defined as ideal hinge joints that are driven by active moments τ_s and τ_e (Ackermann et al., 2015). The assumptions that have been established in the literature pertaining to wheelchair propulsion kinematics include: the shoulder does not move relative to the wheelchair and there is no slip between the ground and the wheel (Ackermann et al., 2014; Ackermann et al., 2015; Leary et al., 2012; Rankin et al., 2010, 2012; Rankin et al., 2011). Anthropometric data (Winter, 2009) was used to determine the body segment lengths, mass, center of mass, and radius of gyration for each segment. The test subject from this experiment had a height of 1.75meters and weight of 75kg. Wheelchair dimensions were obtained from the manual. A generalized coordinate system, q, was developed which is defined as the "angle between the upper arm and the vertical β, the angle between the forearm and the vertical, α, and the horizontal displacement of the wheelchair and shoulder joint, x," as $q = \begin{bmatrix} x & \beta & \alpha \end{bmatrix}$ (Ackermann et al., 2015). As such, the wheelchair-user system is modeled as a closed-loop kinematic chain which has only one degree of freedom. In doing so, the contact between the hand-rim is expressed as:

$$c(x, \beta, \alpha) = 0 \tag{2.1}$$

The Newton-Euler Formalism equation was derived to develop the equations of motion for the wheelchair, "where M is the mass matrix, k is the vector of generalized Coriolis and centrifugal forces, k_g is the vector of generalized forces due to gravity, G transforms the horizontal F_x and vertical F_y components of the pushrim force in generalized forces, H transforms the shoulder moment τ_s and the elbow moment τ_e in generalized forces, and Q transforms the rolling resistance force F_{roll} in generalized force" (Ackermann et al., 2015). Matrices used in this equation can be found in Table 1 of the Appendix.

$$M(q)\ddot{q} + k(q,\dot{q}) = k_G(q) + G(q)\begin{bmatrix} F_x \\ F_y \end{bmatrix} + H(q)\begin{bmatrix} \tau_s \\ \tau_e \end{bmatrix} + Q\left[F_{roll}\right] \tag{2.2}$$

Reconstruction of the motion profile of the wheelchair $(q(t), \dot{q}(t), \ddot{q}(t))$ was used in order to develop the kinematics of the multibody system $(x(t), \dot{x}(t), \ddot{x}(t))$. As such, using the constraint equations, and the first and second order derivatives, the following can be confirmed:

$$\begin{gathered} c_q\dot{q} = 0 \\ c_q\ddot{q} + \dot{c}_q\dot{q} = 0 \end{gathered} \tag{2.3}$$

2.3. **Gaussian Process Regression.** Bayesian inference is a way in which to get a more accurate prediction of data parameters. In this scenario, a probability density $\pi(\theta)$, or a prior distribution, is selected that provides an estimate of what parameter - θ - is expected to be before analyzing the data. From there, a statistical model, $p(x|\theta)$,is selected in a manner that reflects the beliefs of x given ϑ. After analyzing the data $D_n = X_1, ..., X_n$,the beliefs are updated and the posterior distribution, $p(\theta|D_n)$,is calculated (Wasserman & Lafferty, 2014).

Following Bayes' theorem, the posterior distribution can be written as (Wasserman & Lafferty, 2014):

$$p\left(\theta \mid X_1, \ldots, X_n\right) = \frac{p\left(X_1, \ldots, X_n \mid \theta\right)\pi(\theta)}{p\left(X_1, \ldots, X_n\right)} = \frac{\zeta_n(\theta)\pi(\theta)}{c_n} \propto \varsigma_n(\theta)\pi(\theta) \tag{2.4}$$

where $\varsigma_n(\theta) = \prod_{i=1}^{n} p\left(X_1 \mid \theta\right)$, n(ϑ) =i=1np(X1 | ϑ),is the likelihood function of θ and c_n the normalizing constant (evidence) which is expressed as (Wasserman & Lafferty, 2014):

$$c_n = p\left(X_1, \ldots, X_n\right) = \int p\left(X_1, \ldots, X_n \mid \theta\right)\pi(\theta)d\theta = \int \varsigma_n(\theta)\pi(\theta)d\theta \tag{2.5}$$

In summary, when Bayes' theorem is applied, the prior is multiplied by the likelihood function which is then normalized such that posterior $= \frac{\text{likelihood*prior}}{\text{marginal likelihood}}$. This allows the posterior probability distribution to be estimated. A Gaussian random variable can be expressed as $x\ N(\mu, \Sigma)$ where Σ represents the mean, and corresponds to the covariance matrix (Kuss, 2006). Of such, the Gaussian distribution is expressed as:

$$P(x;\mu,\Sigma) = \frac{1}{(2\pi)^{\frac{d}{2}}|\Sigma|} e^{-\frac{1}{2}\left((x-\mu)^{\top}\Sigma^{-1}(x-\mu)\right)} \tag{2.6}$$

Gaussian processes are the "generalization of a Gaussian distribution over a finite vector space to a function space of infinite dimension," or essentially a Gaussian distribution over a function (Rasmussen, 2003). In doing so, the process makes it possible to develop stronger conclusions of parameters based on the data available. Similar to Bayesian inference, Gaussian inference specifies a prior and calculates the posterior from the available data to determine the predictive posterior distribution. As such, the Gaussian process is specified based on its mean $m(x)$ and covariance or kernel function $k(x, x')$, with the former being a vector and the latter being a matrix (Kuss, 2006; Rasmussen, 2003). The covariance matrix K is constructed from the covariance function, $K_{ij} = K(x_i, x_j)$. As such, the covariance function "characterizes the correlations between different points in the process" and is most commonly expressed as the squared exponential kernel where l varies the length and σ defines the height of the kernel (Kuss, 2006; Rasmussen, 2003):

$$K\left(\boldsymbol{x}, \boldsymbol{x}'\right) = \sigma^2 \exp\left(-\frac{\left(\boldsymbol{x}-\boldsymbol{x}'\right)^T\left(\boldsymbol{x}-\boldsymbol{x}'\right)}{2l^2}\right) \tag{2.7}$$

As a result, the Gaussian process is performed over functions and can be expressed through the following equation:

$$f \sim GP(m, k) \tag{2.8}$$

Stochastic behavior is introduced to this process through the individual random variables that are obtained from the Gaussian distribution itself. This means that for every input, x, there is a corresponding random variable, $f(x)$, which is the value of the stochastic function, f (Kuss, 2006). As expressed earlier, by using the methodology applied in Bayesian inference, a specified prior can be applied to Bayes' rule to calculate the posterior distribution. In doing so, the posterior distribution incorporates information from both the dataset and the prior distribution. In this case, however, the likelihood and prior are typically Gaussian.

The Gaussian process prior is specified by the mean and covariance function and is expressed as:

$$f_{\text{pri}}(X_*) \sim GP(m(X_*), k(X_*)) \tag{2.9}$$

Within this prior, previous knowledge about the space function, f, can be integrated through the selection of both the mean and covariance (Rasmussen, 2003). Therefore, based on the training data X, the corresponding observations $f = f(X)$, the test data points X_*, and the infer function values ($f_* = f(X_*)$ the joint distribution can be expressed as: $p(f, f_*|X, X_*) = \mathcal{N}(f; \mu(X), K(X, X))$.

$$\begin{pmatrix} f \\ f_* \end{pmatrix} \sim \mathcal{N}\left(\begin{bmatrix} \mu \\ \mu_* \end{bmatrix}, \begin{bmatrix} K & K. \\ K_*^T & K_{**} \end{bmatrix}\right) \tag{2.10}$$

with $\mu = m(X)$, $\mu = m(X_*)$, $K = K(X, X)$, $K_* = K(X, X_*)$, and $K_{**} = K(X_*, X_*)$.

Based on this information, f_* or $p(f_*|X_*, X, f)$, must be inferred based on the rules for conditioning multivariate Gaussians. For example, when y has a joint Gaussian distribution, the following equation can be expressed as:

$$\boldsymbol{y} = \begin{bmatrix} \boldsymbol{y}_1 \\ \boldsymbol{y}_2 \end{bmatrix} \sim \mathcal{N}\left(\boldsymbol{\mu} = \begin{bmatrix} \boldsymbol{\mu}_1 \\ \boldsymbol{\mu}_2 \end{bmatrix}, \boldsymbol{\Sigma} = \begin{bmatrix} \boldsymbol{\Sigma}_{11} & \boldsymbol{\Sigma}_{12} \\ \boldsymbol{\Sigma}_{21} & \boldsymbol{\Sigma}_{22} \end{bmatrix}\right) \tag{2.11}$$

In addition, the posterior conditional of p(y2 | y1) is expressed as:

$$\begin{aligned} \boldsymbol{y}_2 \mid \boldsymbol{y}_1 &\sim \mathcal{N}\left(\boldsymbol{\mu}_{2|1}, \boldsymbol{\Sigma}_{2|1}\right) \\ \boldsymbol{\mu}_{2|1} &= \boldsymbol{\mu}_2 + \boldsymbol{\Sigma}_{21}\boldsymbol{\Sigma}_{11}^{-1}\left(\boldsymbol{y}_1 - \boldsymbol{\mu}_1\right) \\ \boldsymbol{\Sigma}_{2|1} &= \boldsymbol{\Sigma}_{22} - \boldsymbol{\Sigma}_{21}\boldsymbol{\Sigma}_{11}^{-1}\boldsymbol{\Sigma}_{12} \end{aligned} \tag{2.12}$$

These conditions thus result in the following equation which can be used to compute the expectations for the obtained data:

$$\boldsymbol{f}_* \mid \boldsymbol{f}, \boldsymbol{X}, \boldsymbol{X}_* \sim \mathcal{N}\left(\boldsymbol{\mu}_* + \boldsymbol{K}_*^T\boldsymbol{K}^{-1}(\boldsymbol{f} - \boldsymbol{\mu}), \boldsymbol{K}_{**} - \boldsymbol{K}_*^T\boldsymbol{K}^{-1}\boldsymbol{K}_*\right) \tag{2.13}$$

3. Solution

Based on the kinematic data obtained in the wheelchair module, a Bayesian and Gaussian process regression algorithm was developed in order to estimate the forces and moments applied to the wheel given the three-dimensional motion capture data.

`fitrgp` is a MATLAB function that fits data to a Gaussian process regression (GPR) model. The code below describes how the `fitrgp` function was applied to the data to obtain a Gaussian process regression. In doing so, the model will take the markers from the cameras and return the estimated forces/moments applied to the wheel. `fitrgp` will fit the model by maximizing the marginal log likelihood. Furthermore, the probability equation (below) relates the probability of y_i given the data.

$$P\left(y_i \mid f\left(x_i\right), x_i\right) \sim N\left(y_i \mid h\left(x_i\right)^T \beta + f\left(x_i\right), \sigma^2\right) \tag{3.1}$$

As such, `fitrgp` will "estimate the coefficients β, the noise variance σ^2, and the hyper-parameters, θ, of the kernel function from the data while training the model, the default function is the squared exponential kernel" (Heidkamp, 2016). An usage example of this this function to create the model and estimate the force and moments applied to the wheelchair wheel is presented in the following:

```
% State Variables (Wheelchair Pos, Shoulder and Elbow angles)
x_observed = getStates();
% Force and Moment applied to the wheel
y_observed = getForcesAndMoments();
```

```
% Generate GPR Model
gprMdl = fitrgp(x_observed,y_observed);
% Given observed inputs, predict output
ypred = predict(gprMdl,x_observed);
```

The full code solution is available at: ESC-704-Stochastic-Systems Repository at GitHub.

4. Results

The top three plots in Figure 4 shows the wheelchair position and joint angles (elbow and shoulder). The angle information is solved through basic geometric relationship of the markers position. The last two rows of plots correspond to the collected Force and Moment information of the wheelchair. Plots on the left correspond to the left side of the user and wheelchair, and in the right corresponds to the right side.

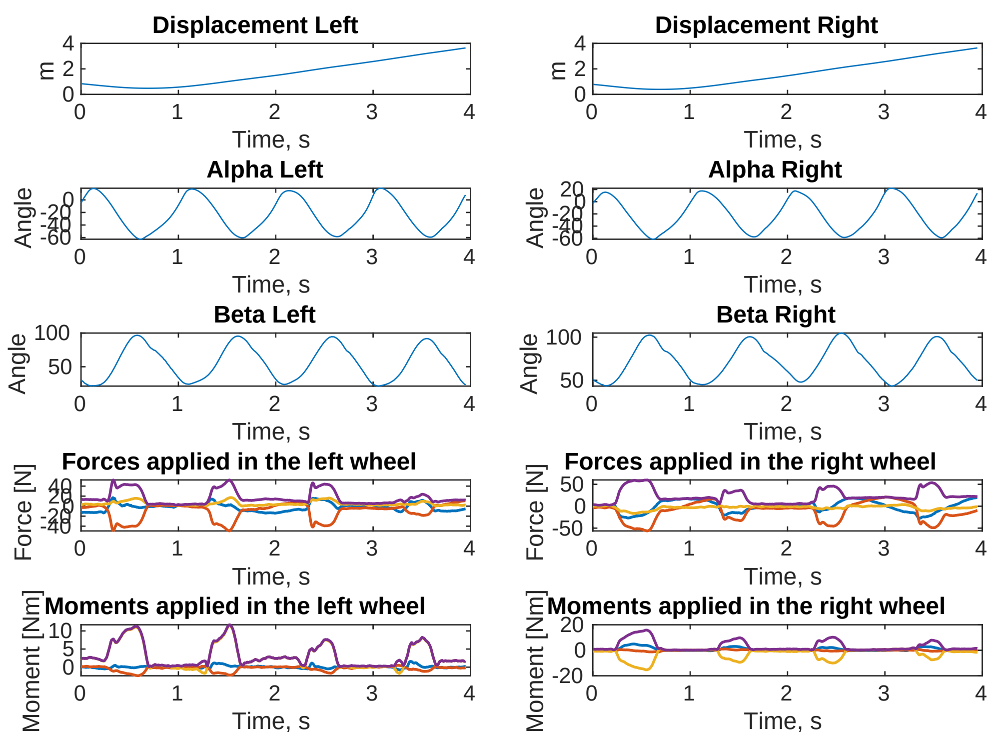

Figure 4. Input and Output Information used for GPR.

From the calculated joint angles depicted in Figure 4, the GRP was able to determine the x and y components of the force and moments applied to the wheelchair. In doing so, the GPR predictions were able to successfully and accurately reflect the kinematics that were measured using the SmartWheel sensor. As demonstrated in Figure 5, the GRP predictions were able to follow the trends of the actual signal even if noisy observations were added to the joint angles. The accuracy of the GRP model is further reiterated by the 95-percent prediction intervals. This shows that the GRP models are 95-percent confident that the GPR predictions fall within this range, thus showing the high degree of accuracy of this methodology.

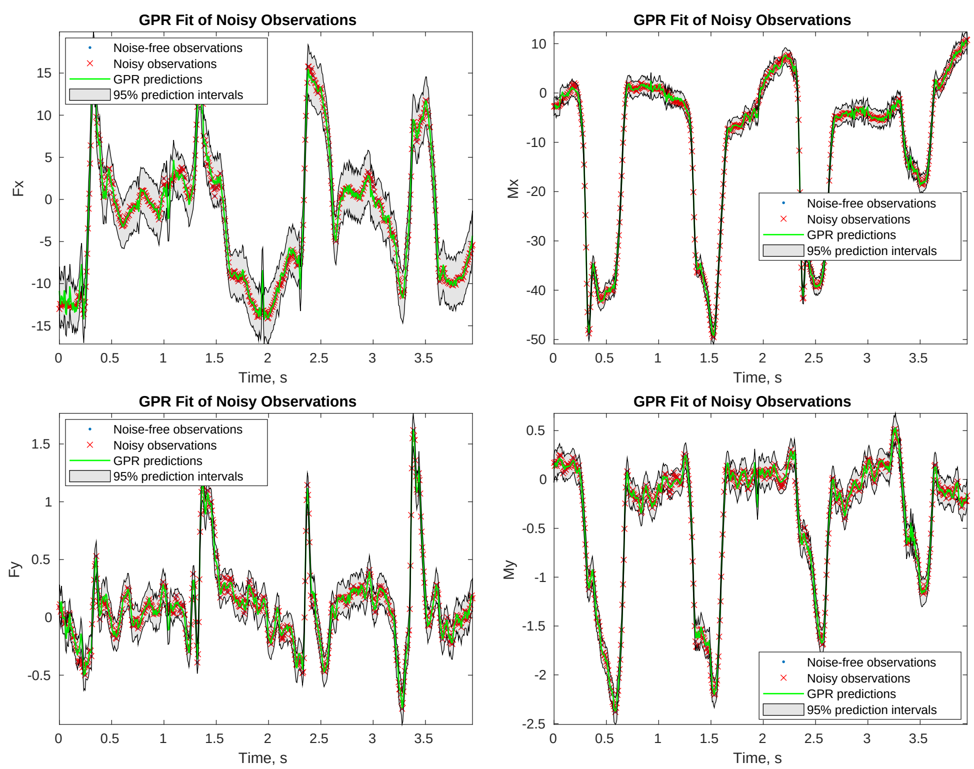

Figure 5. Output results from GPR.

5. Alternative Regression Solvers

Matlab provides a **Regression Learner** Toolbox (The MathWorks, 2021) that helps the task of selecting a regression algorithm. It allows to train and validate several models and compare their validation errors. Then, the developer can choose the best model. The workflow process to train any model is described in Figure 6:

Figure 6. Flow chart for training regression models in the Regression Learner app.

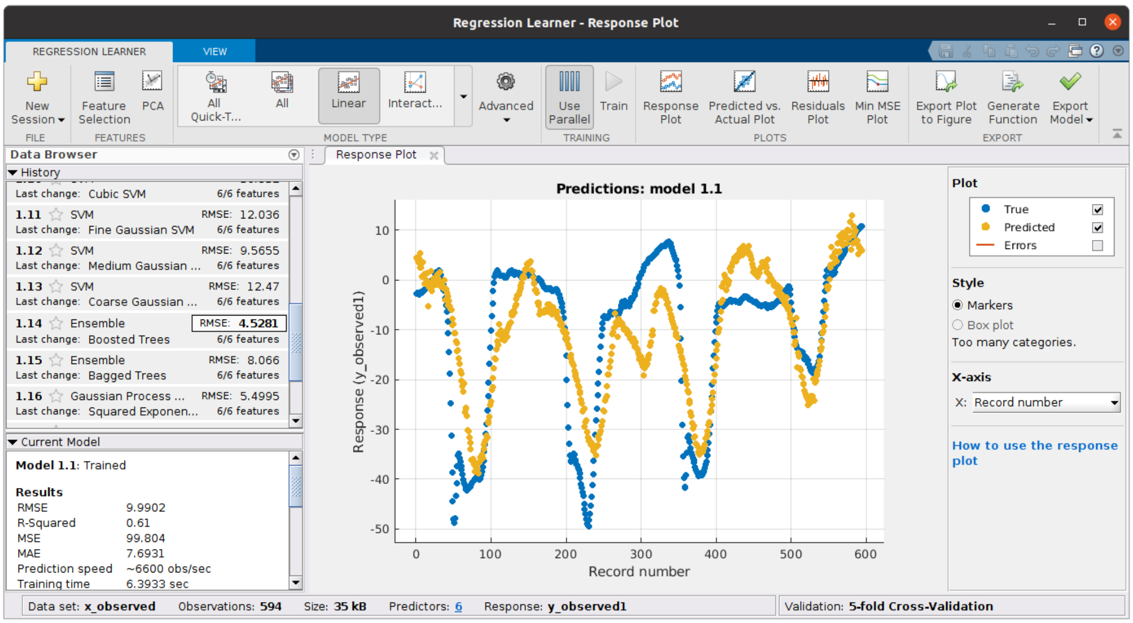

Figure 7. Regression Learner app.

The existent regression model found in Regression Leaner toolbox are:

- **Linear Regression Models:** a fitted regression model that describes the relationship between a response and the corresponding predictors. In doing so, the linearity of the linear regression model describes the linearity of the predictor coefficients. The goal is to minimize the sum of the squared errors.
- **Regression Trees:** a method in which to predict responses for new data using a predictive method through binary splits for regression. In doing so, this model will allow the input variables to be a mixture of categorical and continuous variables. The regression trees will be created when the decision node of the tree contains a test of one of the input variable's value.
- **Support Vector Machines:** the goal of this model is to minimize the coefficients rather than the squared error. This gives the option to define how much error is acceptable within the model and individualizes the hyper-plane which maximizes the margin.
- **Gaussian Process Regression Models:** a model that is non-parametric and based on the Bayesian approach to calculate the probability distribution over all

functions that fit the data. As such, a Gaussian prior will be used to compute the posterior distribution.

- **Ensembles of Trees:** a model that is composed of several regression trees of various weighted combinations. The incorporation of many different regression trees increases the predictive performance of the model.
- **Neural Networks:** a model that uses adaptive weights and has the ability to approximate non-linear patterns in data. This is possible through the utilization of generalized linear models and considering different distribution outcomes.

6. Discussion

Although the GPR models were able to successfully and accurately predict the force and moments applied to the wheelchair, there are some disadvantages to using this regression method. One of the main limitations of this process is that it utilizes all the data and features of the input to perform the prediction. Although in some scenarios this can be advantageous, in instances where the data has excessive noise, the GRP prediction is not able to distinguish between the actual signal and the noise. As such, in trials that had more noise, the regression for the predicted force and moments were skewed and did not closely follow the original signal measurements. Therefore, this demonstrates that although the utilization of GRP can be advantageous in predicting the force and moments applied to the wheelchair based on the 3D motion capture joint angles, it will experience higher degrees of error when more noise is introduced to the signal. To improve the model, the utilization of the EMG signals from the shoulder and arm muscles can be incorporated into the prediction. Determining when muscles such as the rhomboid, biceps, and triceps are activated will provide a better understanding of when the wheelchair propulsion motion is occurring and help distinguish between a muscle contracting and relaxing. Syncing the EMG signals with the shoulder and elbow joint angles will provide a more in depth picture of the propulsion motion and can result in better overall GRP predictions. The magnitude of the EMG signal can also be used to determine the strength of the muscle contraction which can be applied to the force and moment predictions.

7. Conclusion

The 3D motion capture data of the wheelchair propulsion can be used to calculate the joint angles of the elbow and shoulder. A Gaussian regression can be applied to this data to accurately calculate and predict the forces and moments applied to the wheel itself. This is a tremendously useful and advantageous methodology because it allows researchers to rely on 3D motion capture equipment which is common in many biomechanics laboratories instead of the highly expensive wheelchair sensors. By comparing the actual data of the wheelchair sensor to that that was predicted by the Gaussian model, this stochastic methodology can be a reliable and accurate way to obtain the necessary wheelchair kinematics that make it possible to better understand and improve wheelchair design.

References

Ackermann, M., Leonardi, F., Costa, H., & Fleury, A. (2014). Modeling and optimal control formulation for manual wheelchair locomotion: The influence of mass and slope on performance. *5th IEEE RAS/EMBS International Conference on Biomedical Robotics and Biomechatronics*, 1079–1084.

Ackermann, M., Costa, H. R., & Leonardi, F. (2015). A modeling framework to investigate the radial component of the pushrim force in manual wheelchair propulsion. *MATEC Web of Conferences*, *35*, 02008.

Boninger, M. L., Souza, A. L., Cooper, R. A., Fitzgerald, S. G., Koontz, A. M., & Fay, B. T. (2002). Propulsion patterns and pushrim biomechanics in manual wheelchair propulsion. *Archives of physical medicine and rehabilitation*, *83*(5), 718–723.

Cooper, R. A., & Quatrano, L. A. (1999). Research on physical activity and health among people with disabilities: A consensus statement. *Journal of Rehabilitation Research & Development*, *36*(2).

dos Santos, E. G. (2017). Propulsion raw data.

Heidkamp, W. (2016). Predicting the concentration of residual methanol in industrial formalin using machine learning.

Jaimes, K. A. G. (2016). *Avaliação biomecânica de usuários de cadeira de rodas manual* (Doctoral dissertation). Federal University of ABC, Brazil.

Kotajarvi, B. R., Sahick, M. B., An, K.-N., Zhao, K. D., Kaufman, K. R., & Basford, J. R. (2004). The effect of seat position on wheelchair propulsion biomechanics. *Journal of Rehabilitation Research & Development*, *41*.

Kuss, M. (2006). *Gaussian process models for robust regression, classification, and reinforcement learning* (Doctoral dissertation). echnische Universität Darmstadt Darmstadt, Germany.

Leary, M., Gruijters, J., Mazur, M., Subic, A., Burton, M., & Fuss, F. (2012). A fundamental model of quasi-static wheelchair biomechanics. *Medical engineering & physics*, *34*(9), 1278–1286.

Rankin, J. W., Kwarciak, A. M., Richter, W. M., & Neptune, R. R. (2010). The influence of altering push force effectiveness on upper extremity demand during wheelchair propulsion. *Journal of Biomechanics*, *43*(14), 2771–2779.

Rankin, J. W., Kwarciak, A. M., Richter, W. M., & Neptune, R. R. (2012). The influence of wheelchair propulsion technique on upper extremity muscle demand: A simulation study. *Clinical Biomechanics*, *27*(9), 879–886.

Rankin, J. W., Richter, W. M., & Neptune, R. R. (2011). Individual muscle contributions to push and recovery subtasks during wheelchair propulsion. *Journal of biomechanics*, *44*(7), 1246–1252.

Rasmussen, C. E. (2003). Gaussian processes in machine learning. *Summer school on machine learning*, 63–71.

The MathWorks, I. (2021). *Regression learner toolbox*. Natick, Massachusetts, United State. https://www.mathworks.com/help/stats/regression-learner-app.html

Van der Woude, L., Veeger, H., Dallmeijer, A., Janssen, T., & Rozendaal, L. (2001). Biomechanics and physiology in active manual wheelchair propulsion. *Medical engineering & physics*, *23*(10), 713–733.

Veeger, H., Van Der Woude, L., & Rozendal, R. (1991). Load on the upper extremity in manual wheelchair propulsion. *Journal of electromyography and kinesiology*, *1*(4), 270–280.

Wasserman, L., & Lafferty, J. (2014). *Statistical machine learning for structured and high dimensional data* (tech. rep.). CARNEGIE-MELLON UNIV PITTSBURGH PA.

Winter, D. A. (2009). *Biomechanics and motor control of human movement*. John Wiley & Sons.

Wu, G., Van der Helm, F. C., Veeger, H. D., Makhsous, M., Van Roy, P., Anglin, C., Nagels, J., Karduna, A. R., McQuade, K., Wang, X., et al. (2005). Isb recommendation on definitions of joint coordinate systems of various joints for the reporting of human joint motion—part ii: Shoulder, elbow, wrist and hand. *Journal of biomechanics*, *38*(5), 981–992.